Journal of Alloys and Compounds 509 (2011) 3353–3356

Contents lists available at ScienceDirect

Journal of Alloys and Compounds

journal homepage: www.elsevier.com/locate/jallcom

Fabrication of $GdBa_2Cu_3O_{7-x}$ films by TFA-MOD process

L.H. Jin [a,b], Y.F. Lu [a,b,*], W.W. Yan [b], Z.M. Yu [b], Y. Wang [b], C.S. Li [b]

[a] College of Material Science and Engineering, Shaanxi University of Science and Technology, Xi'an 710021, PR China
[b] Northwest Institute for Nonferrous Metal Research, Xi'an 710016, PR China

ARTICLE INFO

Article history:
Received 12 October 2010
Received in revised form 1 December 2010
Accepted 8 December 2010
Available online 15 December 2010

PACS:
74.72.−h
74.78.Bz

Keywords:
Coated conductors
TFA-MOD
$GdBa_2Cu_3O_{7-x}$

ABSTRACT

$GdBa_2Cu_3O_{7-x}$ (GdBCO) films have been deposited on $LaAlO_3$ (LAO) (0 0 l) single crystal substrates by trifluoroacetate metal organic deposition (TFA-MOD) method. The effects of oxygen partial pressure and firing temperature on microstructure and critical properties of GdBCO films were discussed. The phase formation, texture and microstructure of films were characterized by X-ray diffraction and scanning electron microscopy. The oxygen partial pressure was considered to play a great role for formation of impurity phase and *a*-axis oriented grains. The degree of *c*-axis orientation was also influenced by the firing temperature. The highly *c*-axis oriented GdBCO film obtained at 815 °C under an oxygen partial pressure of 100 ppm has a high performance critical current density J_c (77 K, self field) = 1.8 MA/cm^2.

1. Introduction

The trifluoroacetate metal organic deposition (TFA-MOD) has been developed for the preparation of biaxially textured $YBa_2Cu_3O_{7-x}$ (YBCO) layers for coated conductors. The solution-based method is well known as a low-cost process comparing with the physical vapor deposition methods [1,2]. $REBa_2Cu_3O_{7-x}$ superconductors with high critical current density (J_c) in high magnetic field have been intensively researched for the applications of the second-generation superconducting wires. Especially, high quality $GdBa_2Cu_3O_{7-x}$ (GdBCO) films with high J_c in a magnetic field were obtained by pulsed laser deposition (PLD) method [3]. Thus people expect that GdBCO films prepared by MOD should also show strong flux pinning effect in fields. However, in contrast to the richness of the literature on YBCO films, there has been little research on GdBCO films by solution-based techniques.

Recently, Iguchi et al. reported that GdBCO films using the TFA-MOD process exhibited higher T_c and J_c in high magnetic fields compared to YBCO films [4]. Kaneko et al. fabricated GdBCO films on $SrTiO_3$ substrates by an advanced TFA-MOD method [5]. Nakamura et al. also prepared GdBCO films by MOD technique using metal-naphthenates as precursors [6]. There is no more detail about the effects of oxygen partial pressure and firing temperature on the phase formation and texture of GdBCO films. So investigations are needed to reveal the orientation growth of GdBCO films as the functions of firing conditions. In this study, GdBCO films were deposited on $LaAlO_3$ (LAO) (0 0 l) substrates using TFA-MOD method. We investigated the effects of crystallization conditions on the preferential orientation growth and superconducting properties of GdBCO films.

2. Experimental

The precursor solution for GdBCO films was prepared by dissolving the acetates of Gd, Ba and Cu (Gd:Ba:Cu = 1:2:3) in de-ionized water with trifluoroacetic acid. The mixture was continuously refluxed at 80 °C for 4 h and refined under a reduced pressure to yield a blue dry gel. The gel was redissolved in methanol to obtain a solution with a total metal cations concentration of 1.5 mol/L. The solution was coated onto LAO substrates with a spinning rate of 4000 rpm for 2 min. The spin-coated gel films were annealed in two stages in order to produce superconducting films. The gel films were calcined at the temperature up to 400 °C in 3.1% humidified oxygen atmosphere to form oxygen-fluorides films. Subsequently, the GdBCO precursor films were crystallized at various temperatures (805–835 °C) for 2 h in Ar–0.01% O_2 with 4.2% humidity. The oxygen partial pressure was varied in the range of 20–700 ppm. In the last stage the crystallized films were annealed at 450 °C for 4 h in a dry oxygen atmosphere.

Thermal analysis (TA Q1000DSC) were performed under air flow. The phase purity and the texture of GdBCO films were investigated by X-ray diffraction (XRD) using Cu Kα radiations (Rigaku D/MAX2000PC). The morphology of GdBCO films was characterized by scanning electron microscopy (SEM JSM-6460). The critical current density was measured by an inductive method at 77 K.

* Corresponding author at: Northwest Institute for Nonferrous Metal Research, Xi'an 710016, PR China. Tel.: +86 29 86231079; fax: +86 29 86224487.
E-mail addresses: lhjin@c-nin.com (L.H. Jin), yflu@c-nin.com (Y.F. Lu).

0925-8388/$ – see front matter.
doi:10.1016/j.jallcom.2010.12.062

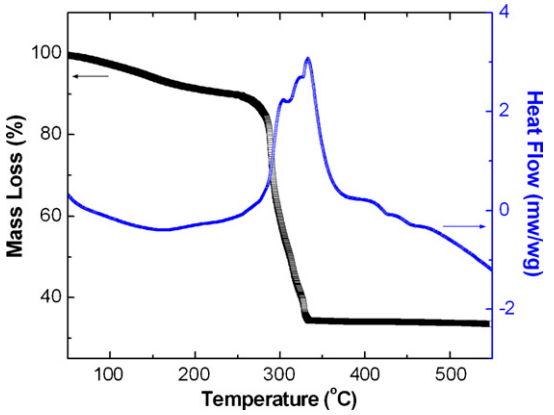

Fig. 1. TG-DSC curves of dry GdBCO gel.

3. Results and discussion

Fig. 1 gives the TG-DSC curves of dry gel of GdBCO precursor solution, in which the sample was heated at 20 °C/min in air. In the temperature range of 250–330 °C, most of the weight loss occurs. We believe that the appearance of three exotherm peaks are derived from the thermal partial decomposition of $Cu(TFA)_2$, $Gd(TFA)_3$ and $Ba(TFA)_2$, respectively. The result is similar to the decomposition behavior of TFA-YBCO gel reported by Dawley et al. [7] and Obradors and co-workers [8]. Hence, the traditional pyrolysis process (less than 10 h) could be used to achieve the decomposition of GdBCO films.

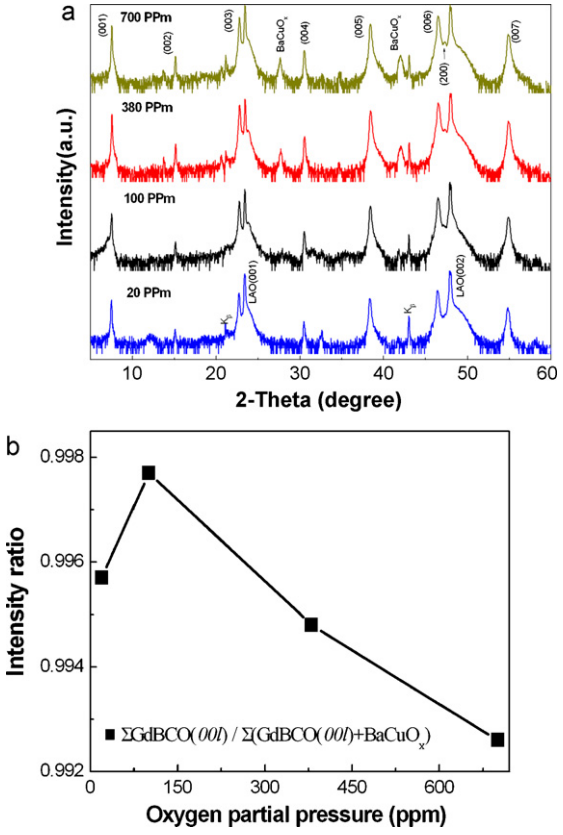

Fig. 2. (a) θ–2θ scans of GdBCO films prepared at 815 °C under various oxygen partial pressures: 20 ppm, 100 ppm, 380 ppm, 700 ppm. (b) The intensity ratio of GdBCO dependent on oxygen partial pressure, (■) $\sum$GdBCO(0 0 l))/$\sum$(GdBCO(0 0 l))+$BaCuO_x$).

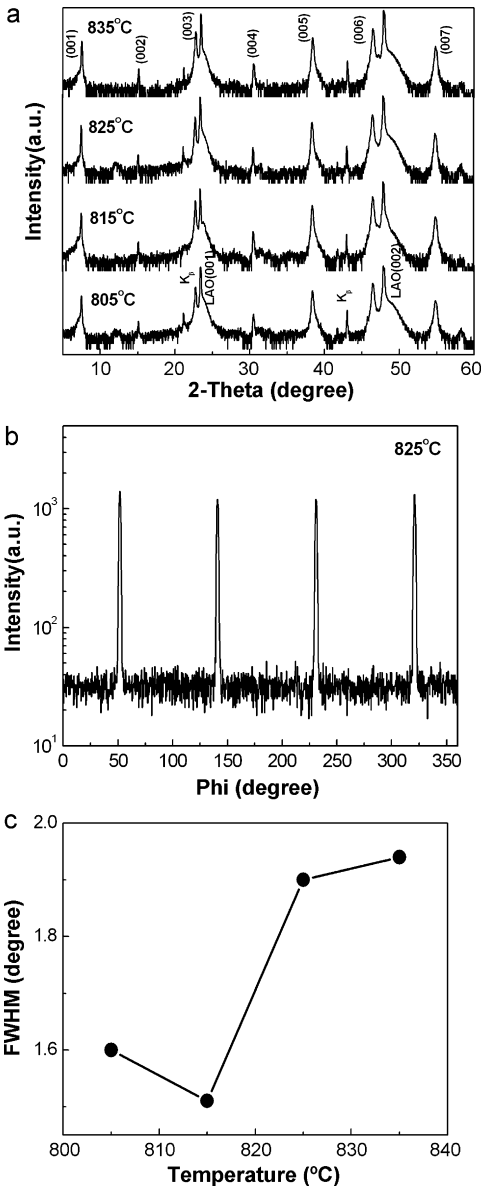

Fig. 3. (a) θ–2θ scans of GdBCO films prepared at different temperatures under 100 ppm oxygen atmosphere. (b) The typical phi-scan of GdBCO (1 0 2) at the firing temperature of 825 °C. (c) The FWHM values dependent on temperature.

It is equally important to optimize the crystallization parameters for the growth of GdBCO film, such as the oxygen partial pressure and the firing temperature. The low oxygen partial pressure is beneficial to produce *a*-axis free GdBCO films. The XRD patterns for GdBCO films fired at 815 °C under the oxygen partial pressures between 20 and 700 ppm are shown in Fig. 2(a). It can be seen that all films have *c*-axis preferred orientations, except that minor impurity phase $BaCuO_x$ peaks exist in the films crystallized under high oxygen partial pressure (380 ppm, 700 ppm). On the other hand, weak (2 0 0) peak is observed in XRD patterns of the film crystallized under 700 ppm oxygen partial pressure. The (2 0 0) diffraction peak comes from the *a*-axis oriented grains and the intensity of the (2 0 0) peak can be drastically suppressed with decreasing the oxygen partial pressure. The effect of oxygen partial pressure on the *a*-axis oriented grains of GdBCO film is similar to that of SmBCO film [9]. Fig. 2(b) shows the peak intensity ratio of GdBCO films crystallized at 815 °C as a function of oxygen partial pressure. The estimation of peak intensity ratio was calculated by using the following equa-

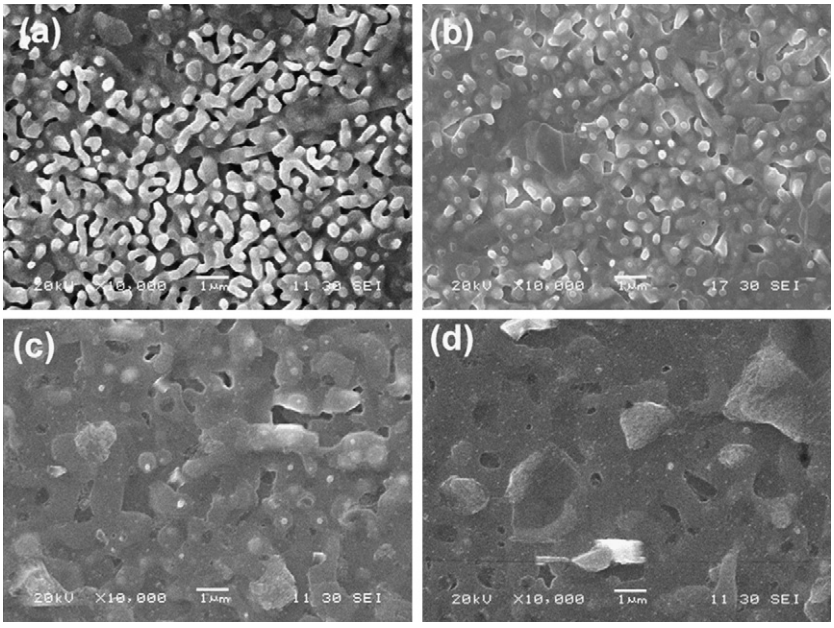

Fig. 4. SEM images of GdBCO films on LAO (1 0 0) substrates fired at different temperatures: (a) 805 °C, (b) 815 °C, (c) 825 °C and (d) 835 °C.

tion: intensity ratio = $\sum$GdBCO(0 0 l)/$\sum$(GdBCO(0 0 l) + $BaCuO_x$). The intensity ratio values depend strongly on the oxygen partial pressure and decrease in proportion to oxygen partial pressure in the range of 100–700 ppm, indicating that the phase purity of *c*-axis orientation grains decreases with increasing the oxygen partial pressure. Especially in case of 100 ppm, the amount of *c*-axis oriented GdBCO grains reaches a maximum.

Fig. 3(a) shows the θ–2θ scans of GdBCO films fired at different temperatures between 805 °C and 835 °C under 100 ppm oxygen partial pressure. It can be seen that the patterns of all films consist of GdBCO (0 0 l) peaks and no second impurity phase is observed. The phi-scans of GdBCO (1 0 2) were carried out to characterize the in-plane texture of the films. Fig. 3(b) shows one typical phi-scan of the film at the firing temperature of 825 °C. As shown in Fig. 3(c), the full-width at half maximum (FWHM) values of in-plane textures are 1.6°, 1.51°, 1.9° and 1.94° for the samples prepared at the firing temperatures of 805 °C, 815 °C, 825 °C and 835 °C, respectively. The FWHM values do not vary significantly with temperatures in the range of 805–835 °C. The FWHM values of the (1 0 2) peak are close to that of TFA-YBCO films grown on other perovskite buffer layers [10]. It can be confirmed that the sharpest texture of GdBCO film was obtained at 815 °C. Fig. 4 shows the SEM images of GdBCO crystallized at various temperatures under 100 ppm oxygen partial pressure. All the films show the crack-free surface without any *a*-axis oriented grains, while there are significant differences in the surface morphology. The pores are observed in Fig. 4(a). The microstructure of GdBCO films becomes denser and the grains grow largely with increasing the firing temperature.

The J_c values of GdBCO films at the firing temperatures are shown in Fig. 5. The J_c reduces with the firing temperature from 815 °C to 835 °C. The trend is similar to the one of TFA-YBCO reported by Jee et al. and TFA-SmBCO reported by Mitani et al. [11,12]. As the firing temperature increases, the J_c reaches a maximum value (1.8 MA/cm^2) at 815 °C, and then decreases when the firing temperature further increases. These results are corresponding to the former results in Fig. 3. The J_c value is 1.62 MA/cm^2 for the GdBCO film prepared at 805 °C, and it is slightly larger than the J_c of 1.55 MA/cm^2 for the sample prepared at 825 °C. It is seen in Fig. 3(c) that the FWHM value (1.6°) of the film prepared at 805 °C is lower than that (1.9°) of the film prepared at 825 °C. This suggests that the

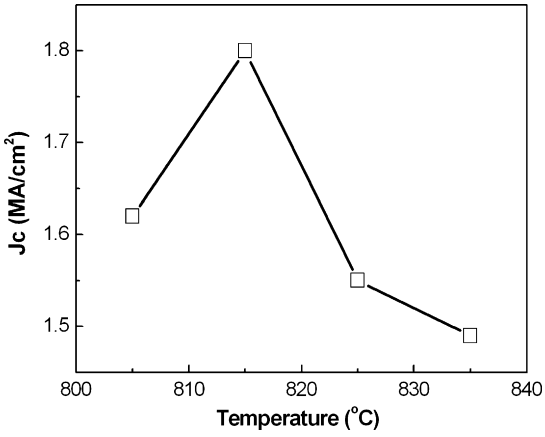

Fig. 5. The J_c values of GdBCO films fired at 805–835 °C.

change of J_c is partially related to the texture degree of the GdBCO films. On the other hand, the film morphology is another factor to influence the J_c for the films. We notice that the porous structure of the fine grains for the sample prepared at 805 °C is apparently not useful for the high J_c and the connectivity among the large plate-like grains for the sample prepared at 825 °C should become worse, resulting in the lower J_c as shown in Fig. 5. Based on the XRD pattern and SEM images, we believe that the highest J_c value is due to the formation of pure GdBCO phase and strong biaxial texture for the sample prepared at 815 °C.

It has been proposed that the YBCO layer heteroepitaxially nucleates at the substrate/precursor interface if the heat treatment conditions are optimal. With increasing heat treatment time, the thickness of the crystallized YBCO layer continues to increase with new grains homoepitaxially nucleating on the underlying YBCO grains and growing laterally [13]. Here the TFA-GdBCO film also starts to nucleate and grow from the interface between LAO and GdBCO layers. The nucleation and growth are influenced by the oxygen partial pressure and the firing temperature. At a given temperature, the low oxygen partial pressure promotes the *c*-axis epitaxy and suppresses the formation of the impurities phase. This

behavior is accounted for the enhanced oxygen-vacancy-induced cation diffusion process at low oxygen pressures [14]. However, the *a*-axis grains tend to form at high temperature at the constant of oxygen partial pressure (100 ppm). The thermodynamic behavior of GdBCO grain formation is related to the heat treatment conditions of the amorphous precursors. When the firing temperature increases, the driving forces become larger than that in the low firing temperature. The increased driving force at the high firing temperature will lead to a faster growth of the *a*-axis grains due to a larger growth rate of the *a*-axis grains than that of the *c*-axis grains [15]. The texture of *c*-axis oriented grains becomes slightly worse under a high driving force condition. At the same time, the very weak peak of *a*-axis oriented grains is observed in XRD pattern of GdBCO films with increasing the firing temperature. Hence, the texture degradation of *c*-axis oriented grains has a correlation with the formation of *a*-axis oriented grains. It is difficult to completely eliminate the nucleation and growth of nanocrystals in the amorphous phase [14]. The nucleation and growth of *a*-axis grains may happen in the amorphous phase. Once the *a*-axis grains are formed, the texture and the J_c of GdBCO films become worse. Therefore, the firing temperature window should be controlled to increase the degree and percentage of *c*-axis oriented grains in the Gd-based system.

4. Conclusion

We have studied the effects of oxygen partial pressure and firing temperature on microstructure and critical properties of GdBCO film prepared by TFA-MOD method. The low oxygen partial pressure is required to successfully obtain GdBCO films without impurity phases and *a*-axis oriented grains. The texture degree of GdBCO film is also influenced by the firing temperature. High performance J_c (77 K, self field) = 1.8 MA/cm^2 has been demonstrated for the highly *c*-axis oriented GdBCO films obtained at 815 °C within oxygen partial pressure of 100 ppm.

Acknowledgements

This work was financially supported by the National Natural Science Foundation of China (no.50872115), the National High Technology Research and Development Program (no. 2008AA03Z201) and the Graduate Innovation Fund of Shaanxi University of Science and Technology.

References

[1] M.W. Rupich, D.T. Verebelyi, W. Zhang, T. Kodenkandath, X. Li, Mater. Res. Soc. Bull. 29 (2004) 572.
[2] X. Obradors, T. Puig, A. Pomar, F. Sandiumenge, N. Mestres, M. Coll, A. Cavallaro, N. Romà, J. Gázquez, J.G. González, O. Castaño, J. Gutierrez, A. Palau, K. Zalamova, S. Morlens, A. Hassini, M. Gibert, S. Ricart, J.M. Moretó, S. Piñol, D. Isfort, J. Bock, Supercond. Sci. Technol. 19 (2006) S13.
[3] N. Chikumoto, S. Lee, K. Nakao, K. Tanabe, Physica C 469 (2009) 1303.
[4] T. Iguchi, T. Araki, Y. Yamada, I. Hirabayashi, H. Ikuta, Supercond. Sci. Technol. 15 (2002) 1415.
[5] A. Kaneko, H. Fuji, R. Teranishi, Y. Tokunaga, J.S. Matsuda, S. Asada, K. Murata, T. Honjo, T. Izumi, Y. Shiohara, T. Goto, A. Yoshinaka, A. Yajima, Physica C 412–414 (2004) 926.
[6] T. Nakamura, R. Kita, O. Miura, A. Ichinose, K. Matsumoto, Y. Yoshida, M. Mukaida, S. Horii, Physica C 463–465 (2007) 540.
[7] J.T. Dawley, P.G. Clem, T.J. Boyle, L.M. Ottley, D.L. Overmyer, M.P. Siegal, Physica C 402 (2004) 143.
[8] K. Zalamova, N. Romà, A. Pomar, S. Morlens, T. Puig, J. Gázquez, E.A. Carrillo, F. Sandiumenge, S. Ricart, N. Mestres, X. Obradors, Chem. Mater. 402 (2006) 143.
[9] G.M. Shin, D.J. Kim, K.J. Song, C. Park, S.H. Moon, S.I. Yoo, IEEE Trans. Appl. Supercond. 17 (2007) 3561.
[10] A. Pomar, M. Coll, A. Cavallaro, J. Gázquez, J.C. González, N. Mestres, F. Sandiumenge, T. Puig, X. Obradors, J. Mater. Res. 21 (2006) 1106.
[11] Y.A. Jee, B. Ma, V.A. Maroni, M. Li, B.L. Fisher, U. Balachandran, Supercond. Sci. Technol. 14 (2001) 285.
[12] A. Mitani, R. Teranishi, K. Yamada, N. Mori, M. Mukaida, T. Kiss, M. Inoue, Y. Shiohara, T. Izumi, K. Nakaoka, J. Matsuda, Physica C 468 (2008) 1546.
[13] T.G. Holesinger, L. Civale, B. Maioro, D.M. Feldmann, J.Y. Coulter, D.J. Miller, V.A. Maroni, Z. Chen, D.C. Larbalestier, R. Feenstra, X. Li, Y. Huang, T. Kodenkandath, W. Zhang, M.W. Rupich, A.P. Malozemoff, Adv. Mater. 20 (2008) 391.
[14] J. Lian, H. Yao, D. Shi, L. Wang, Y. Xu, Q. Liu, Z. Han, Supercond. Sci. Technol. 16 (2003) 838.
[15] K. Nishizono, N. Mori, K. Ogi, J. Japan. Inst. Met. 62 (1998) 557.